(29) AN EXPERIMENTAL STUDY ON ELASTIC-PLASTIC BEHAVIORS AND BENDING STRENGTHS OF CIRCULAR CFT COLUMN BASES WITH BUILT-IN HIGH STRENGTH REINFORCEMENTS

Qiyun QIAO [1], Akihiko KAWANO [2], Yasunori NAKAMURA [3]

[1]Member of AIJ, Doctoral candidate, School of Human-Environment Studies, Kyushu University
(10-1, Hakozaki 6, Higashi-ku, Fukuoka, 812-851, Japan)
E-mail:qiao_08g@web5.arch.kyushu-u.ac.jp
[2]Member of AIJ, Professor, Faculty of Human-Environment Studies, Kyushu University
(10-1, Hakozaki 6, Higashi-ku, Fukuoka, 812-851, Japan))
E-mail:kawano@arch.kyushu-u.ac.jp
[3]Member of AIJ, Nippon Steel Engineering CO.,LTD
(20-1 Shintomi, Futtsu City, Chiba Pref. 293-8511, Japan)
E-mail:nakamura.yasunori1@nsc-eng.co.jp

In this study, the authors proposed a new exposed-type column base which is a circular exposed-type CFT column base with built-in high strength reinforcements (CFTR column base). The base plate and anchor bolts were omitted in this CFTR column base, but the high strength reinforcements were inserted from the CFT column to the foundation. A total of six specimens was fabricated and tested. Parameters for the tests were as follows: (1) axial force ratio, (2) concrete strength, (3) built-in reinforcements, and (4) shear reinforcement ratio. The specimens were tested under reversed cyclic lateral loads while subjected to a constant axial load. The elastic-plastic behaviors, the stress transfer mechanism and the bending strengths of the column bases were investigated. The test results indicated that the exposed-type CFTR column bases have excellent seismic performances and are applicable in practical structural design.

Key Words *: CFTR Column Bases, High Strength Reinforcements, Stress Transfer Mechanism, Elastic-Plastic Behaviors, Bending Strengths*

1. INTRODUCTION

Structures composed of Concrete Filled Steel Tubular with built-in Reinforcements (CFTR) columns and steel-shaped beams have satisfactory fire resistant performance, in comparison with those of usual Concrete Filled Steel Tubular (CFT) columns. Also, according to the limited studies on mechanical performance of the CFTR structures[1),2)], it is proved that the built-in reinforcements can work positively with the steel tubes and the concrete, and the compact column sections may be achieved.

However, research on mechanical performance of the CFTR structures, especially the CFTR connections, is insufficient and unsystematic. Hence, since 2006, our research group started a serial research which contains the experimental and analytical studies on mechanical performance of the CFTR connections. Until now, a pull-out test of CFTR column joint[3)], a pure bending test of CFTR column joint[4)], and a bending-shear test of square CFTR column base[5)] have been done.

Thus far, few studies has carried out on the circular CFTR column base connections. Therefore, the authors conducted an experimental study on the non base-plate type circular CFTR column base connection which is one part of the serial research on the CFTR connections.

Generally, an exposed-type CFT column base consists of a base plate and anchor bolts to connect

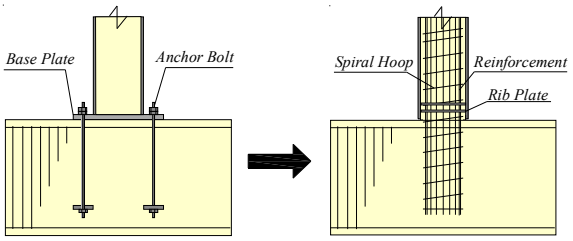

(a) CFT column base (b) CFTR column base

Fig.1 Exposed-type column base

with the foundation, as shown in Fig.1(a). On the other hand, in this study [Fig.1(b)], the base plate and the anchor bolts are totally omitted as structural system, but the built-in reinforcements are inserted through the CFT column to the foundation. A clearance is located between the steel tube and the foundation concrete, which means the steel tube does not touch the foundation concrete. Hence, the cross section of the CFTR column base is the RC cross section composed of the infilled concrete and the built-in reinforcements.The rib plates, which work as the mechanical shear keys between the steel tubes and infilled concrete, are welded inside of the steel tube near the foundation. The effect of the rib plates in stress transfer has already been proved to be good in the previous research[3]. Hence, in this study, instead of the usual base plate and anchor bolts, the built-in reinforcements and the rib plates are expected to act the main role in the stress transfer from the steel tube to the foundation concrete.

With respect to the buildings such as warehouses with long span, the axial loads of the columns should be considered prior to the bending moments of the columns in structural design. When CFT columns are used in such buildings, in order to carry the axial loads, the concrete cross sections of the columns need to be large. Meanwhile, the thin wall steel tubes surround the concrete may be applicable to the economic consideration. Therefore, the steel tubes with a large diameter-to-thickness ratio of 97.5 are used in this study.

Table 1 Summary of test specimens

Specimen		Axial Force Ratio※1	Steel Tube※2			Concrete	Built-in Reinforcements		Spiral Hoop (SD295)
			Grade	Dim.(mm)	D/t		Grade	Quantity	
No.1	C-16M0.2-0.25	0.25	SKK490	φ390×4	97.5	Fc36	USD590	16-D19	0.2%(D6@90)
No.2	C-16M0.2-0.45	0.45							
No.3	C-16M0.2-0.10	0.10							
No.4	C-16H0.2-0.45	0.45				Fc60			
No.5	C-8M0.2-0.25	0.25				Fc36	USD685	8-D19	
No.6	C-16M0.1-0.25	0.25					USD590	16-D19	0.1%(D6@180)

※1. Axial force ratio was decided by the compressive strength of the CFT column
※2. φ 390 × 4 steel tube was fabricated from the φ 400 × 9 steel tube (SKK490 specified in JIS)

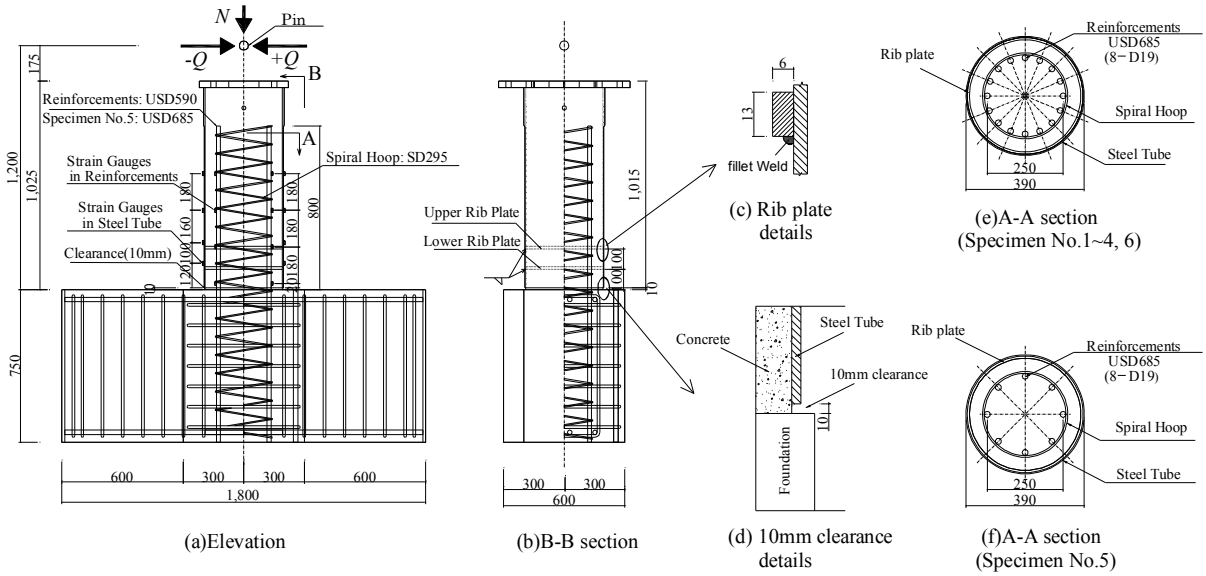

Fig.2 Details of the specimens

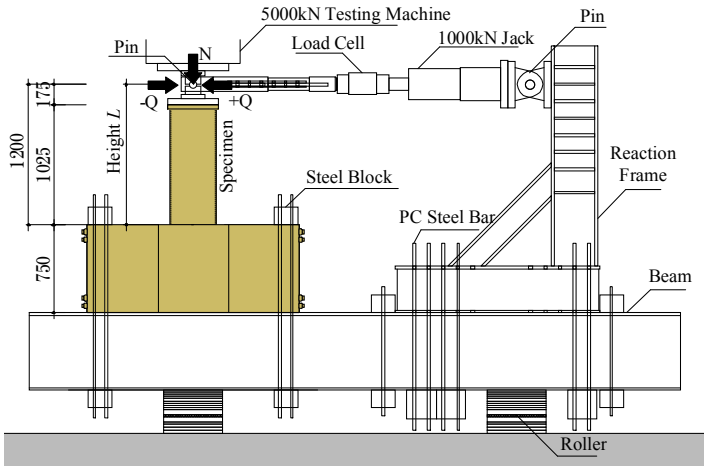

Fig.3 Test setup

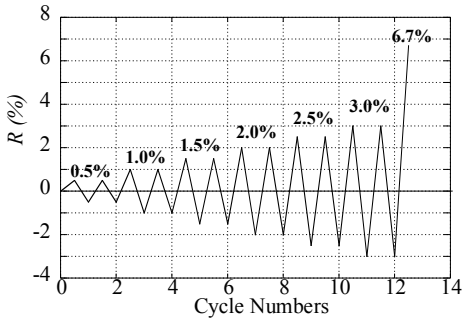

Fig.4 Loading program

Table 2 Steel material properties

Dimension	Type	Specimen	Yield Stress (N/mm^2)	Tensile Stress (N/mm^2)	Yield Strain(%)	Yield Ratio	Young's Modulus (N/mm^2)
○390×4	SKK490	No.1, 2	446	591	0.23	0.75	1.94×10^5
		No.3	409	527	0.22	0.78	1.90×10^5
		No.4	428	550	0.22	0.78	1.96×10^5
		No.5, 6	431	550	0.22	0.78	1.94×10^5
D19	USD590	No.1, 2	625	843	0.32	0.74	1.92×10^5
		No.3, 4, 6	643	863	0.33	0.74	1.95×10^5
	USD685	No.5	740	914	0.37	0.81	2.00×10^5
D6	SD295	All Specimens	386	545	0.21	0.71	1.81×10^5

Table 3 Concrete properties

Specimen		σ_y (N/mm^2)	Young's Modulus (N/mm^2)
No.1	C-16M0.2-0.25	32.8	3.93×10^4
No.2	C-16M0.2-0.45	33.6	3.87×10^4
No.3	C-16M0.2-0.10	31.3	3.21×10^4
No.4	C-16H0.2-0.45	61.4	4.71×10^4
No.5	C-8M0.2-0.25	32.0	3.54×10^4
No.6	C-16M0.1-0.25	34.8	3.48×10^4

The purpose of this study is to investigate the elastic-plastic behaviors, the stress transfer mechanism and the bending strength estimations of the CFTR column bases experimentally.

2. SPECIMENS

Table 1 shows the summary of the test specimens. Figs.2(a) to (f) show the details of the specimens. The high strength reinforcements (USD590 and USD685) were inserted through the CFT column to the foundation concrete. The anchorage length of the built-in reinforcements inside the CFT column was 800mm, which was thought as the enough length to avoid the slip of the built-in reinforcements. As shown in Fig.2(e), the built-in reinforcements were arranged to make the strengths of the CFT columns and the strengths of the CFTR column bases (RC cross section) the same. However, as for specimen No.5, the built-in reinforcements were arranged to make the strength of the CFTR column base smaller than that of the CFT column, as shown in Fig.2(f). The circular steel tube (ϕ 390×4, which was fabricated from ϕ 400×9, SKK490 specified in JIS) with a large diameter-to-thickness ratio of 97.5 were adopted. The mechanical rib plates (FB 6×13, SS400 specified in JIS), which included the upper rib plate and the lower rib plate, were welded inside of the steel tube near the foundation [Figs.2(c)]. A 10mm clearance was located between the steel tube and the foundation[Figs.2(d)]. In this way, the stress was ensured to transfer from the steel tube to the foundation via the rib plates and the built-in reinforcements, but not from the steel tube to the foundation directly. In other words, the stress in the steel tube was firstly transferred to the infilled concrete by the rib plates, then transferred from the infilled concrete to the built-in reinforcements by the bond, and finally transferred to the foundation.

A total of six specimens was fabricated. The parameters for the test were:

(1) Axial force ratio: n =0.10, 0.25, 0.45

where, $n=N/N_u$. N is the axial load and N_u is the critical axial strength as defined below.

A_s : Cross sectional area of the steel tube
σ_y : Yield stress of the steel tube
A_c : Cross sectional area of infilled concrete
$_c\sigma_B$: Maximum stress of the infilled concrete
(2) Concrete design strength: F_c =36, 60 N/mm^2
(3) Built-in reinforcements:
16-D19 (USD590), 8-D19 (USD685)
(4) Shear reinforcement ratio: P_w=0.2%, 0.1%

In the nomenclature for identifying specimen types, the first character(C) represents the circular tube, the first number(16, 8) represents the quantity of the reinforcements, the second character(M, H) represents the concrete strength, the second number(0.2,0.1) represents the shear reinforcement ratio and the final number(0.10, 0.25, 0.45) means the axial force ratio.

Tables 2 and 3 show the steel material and concrete properties.

3. TEST PROCEDURE

Test setup is shown in Fig.3. The reversed cyclic horizontal loads Q were applied by a 1000kN capacity hydraulic jack and the constant axial load N was maintained by a 5000kN capacity universal test machine. As shown in Fig.4, the joint translation angle R ($R=u/L$, where u denotes the lateral displacements and L is the distance from the surface of the foundation to the horizontal loading point) was taken from ±0.5% to ±3.0%, with two cycles in each amplitude of the R. After these loading procedures, the Q was loaded monotonically until 6.7% of the R, which is the limit of the loading apparatus.

The longitudinal strain gauges were used in the reinforcements and steel tubes. The locations of the strain gauges are shown in Fig.2(a). The lateral displacements of the loading point and vertical displacements of the bottom part of the steel tubes were measured by the displacement transducers.

4. TEST RESULTS AND INVESTIGATIONS

(1) Elastic-Plastic behaviors (M- θ relationships)

Figs.5(a) to (f) show the relationships between the bending moment M at the column base and the rotation angle of the column base θ. The symbol $\triangledown$ implies the yielding of the built-in reinforcements. The horizontal dashed lines in Fig.5 represent the calculated ultimate bending strengths of the CFT columns (without built-in reinforcements), the horizontal solid lines represent the calculated ultimate bending strengths of the CFTR column bases. Here, the bending strengths of the CFTR column bases are calculated as the RC section composed of infilled concrete section and built-in reinforcements.

In Fig.5, it is observed that for all the specimens, the peak of the M in each hysteresis loop increases as the amplitude of the θ increases. the hysteretic characteristics are proved to be stable. Even when the θ reaches around 6%, no degradation occurs for all specimens, except No.4 [C-16H0.2-0.45, Fig.5(d)]. As for No.4, the M reaches the maximum when the θ is around 5.0%. From above, the deformation behaviors of the circular CFTR column bases are proved to be excellent.

With respect to all specimens, the experimental bending strengths reach the calculated ultimate strengths of the CFTR column bases.

The influences of the test parameters on the hysteretic loops are shown in Figs.6(a)-(d), the investigations are as follows:

a)Influence of the axial force ratio (n)

Fig.6(a) compares the results of specimens No.1(n=0.25), No.2(n=0.45) and No.3(n = 0.10). The M increases with the increase in the axial force ratio. This can be considered as the result that when the axial force ratio increases, the resisting moment of the concrete also increases. Also, the behaviors are stable for the specimens in Fig.6(a) despite the differences in the axial force ratio.

b)Influence of the concrete strength

Fig.6(b) compares the results of specimens No.2 (C-16M0.2-0.45) and No.4 (C-16H0.2-0.25). The only difference between No.2 and No.4 is the concrete strength. The cylinder strength is 33.6N/mm^2 for No.2, while 61.4N/mm^2 for No.4. It is confirmed that the higher the concrete strength is, the higher the bending strength of the CFTR column base becomes. Also, it is confirmed that the hysteretic loops for both specimens are stable.

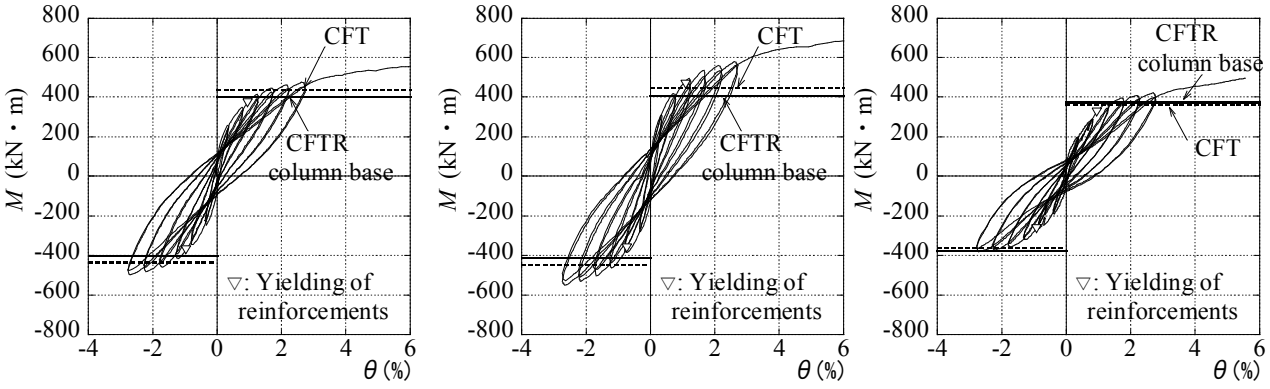

(a)No.1:C-16M0.2-0.25 (b)No.2:C-16M0.2-0.45 (c)No.3:C-16M0.2-0.10

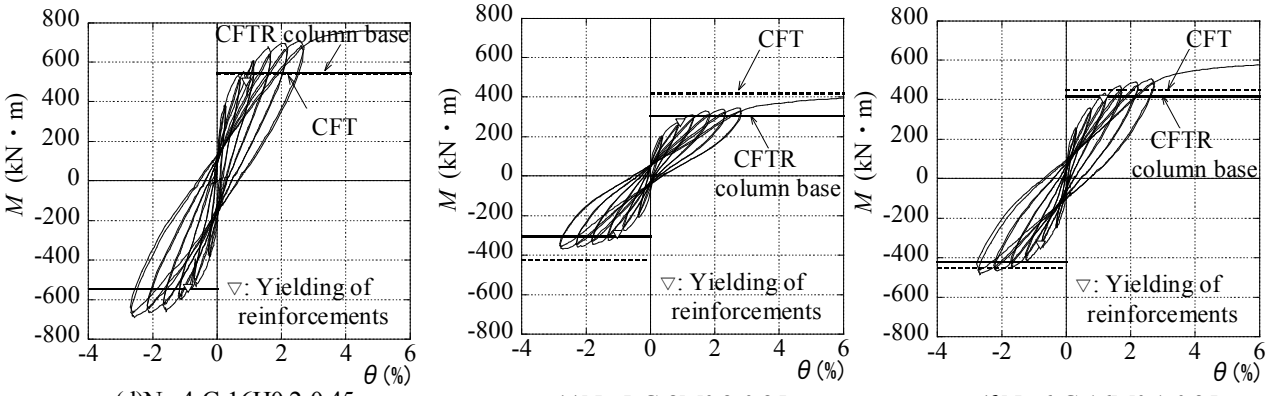

(d)No.4:C-16H0.2-0.45 (e)No.5:C-8M0.2-0.25 (f)No.6:C-16M0.1-0.25

Fig.5 M-θ relationships

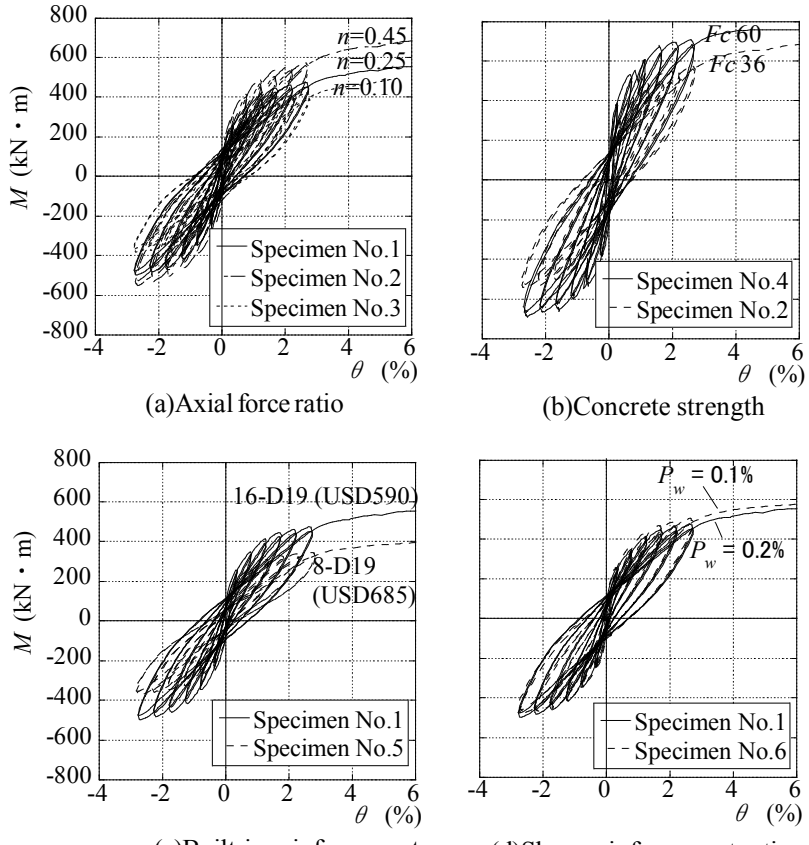

(a)Axial force ratio (b)Concrete strength

(c)Built-in reinforcements (d)Shear reinforcement ratio

Fig.6 Influences of the test parameters

(a) Bending compression side

(b) Bending tension side

Fig.7 Photographs of failures

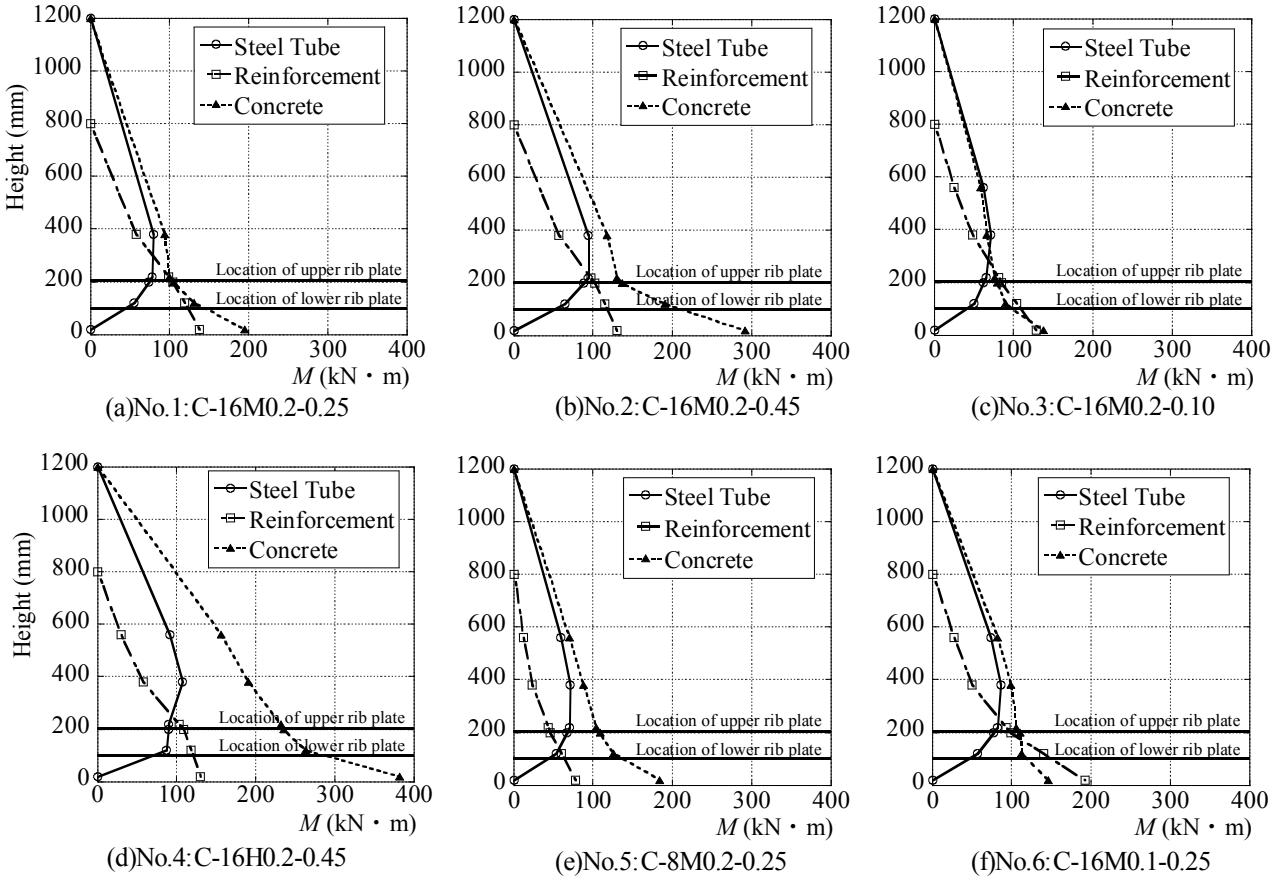

Fig.8 Share conditions of the bending moments

c)Influence of the built-in reinforcements

The Influence of the of specimens No.1(C-16M0.2-0.25) and No.5(C-8M0.2-0.25) are compared in Fig.6(c). As for specimen No.5, the bending strength is smaller than that of specimen No.1 because the strength of the built-in reinforcements is designed to be smaller than that of specimen No.1. The stable behaviors are shown for both specimens in Fig.6(c).

d)Influence of shear reinforcement ratio (p_w)

Fig.6(d) compares the results of specimens No.1(p_w =0.2%) and No.6(p_w=0.1%) which are different only in the shear reinforcement ratio. As for specimen No.6, the material strengths of the built-in reinforcements and concrete of are a little bit higher than those of No.1, as shown in Table 2 and 3. If considering the effect of the differences in material strengths, although the specimens are limited, from Fig.6(d), it can be judged that the shear reinforcement ratio hardly affect the strength nor the hysteretic characteristics.

(2) Fracture mode

Figs. 7(a), (b) show examples (No.2, C-16M0.2-0.45) of the typical fracture mode. The damage is concentrated at the 10mm clearance part between the CFT column and the foundation concrete. The bottom of the steel tube in the bending compression side slightly sink into the surface of the foundation [Fig.7(a)]. While in bending tension side, the cracks are found in the concrete of the 10mm clearance part when the *R* is around 1.0%, and the cracks increases with the increase of the *R* [Fig.7(b)].

(3)Stress transfer mechanism

According to the longitudinal strains in the steel tubes and reinforcements, the bending moment shares of the steel tubes, reinforcements and concrete are calculated when the joint translation angle *R* is 1.0%. The stresses shared by the steel tubes and reinforcements are calculated by multiplying the longitudinal strains by the measured elastic modulus of the steel tube and reinforcements. The Bernoulli-Euler's hypothesis is adopted in the calculation. The concrete contributions are calculated by subtracting the bending moments of the steel tubes and

reinforcements from the total applied bending moments.

Figs.8(a)-(f) show the share conditions of the bending moments when the joint translation angle R is 1.0%. In the figures, the height 0mm represents the surface of the concrete foundation and the height 1200mm represents the height of the loading point. The horizontal solid lines show the locations of the rib plates. Since the steel tubes does not touch the foundation concrete, the bending moments of the steel tubes at 0mm are taken as 0. From the height 400mm to 0mm, the bending moments shared by the steel tubes decreases gradually. This illustrates that the stresses in the steel tubes are transferred to the infilled concrete gradually by the rib plates.

The influences of the test parameters on the share conditions of the bending moments are as follows:

a)Influence of the axial force ratio (n)

When comparing the results of specimens No.1 [n=0.25, Fig.8(a)], No.2 [n=0.45, Fig.8(b)] and No.3 [n=0.10, Fig.8(c)], it is confirmed that the moments shared by the concrete increases with the increase in the axial force ratio n.

b)Influence of the concrete strength(F_c)

The comparison between specimens No.2 [F_c =36N/mm^2, Fig.8(b)] and No.4 [F_c=60N/mm^2, Fig.8(d)] indicates that the bending moment shared by the concrete is higher if the concrete strength is higher.

c)Influence of the built-in reinforcements

When comparing the results of specimen No.1 [C-16M0.2-0.25, Fig.8(a)] and No.5 [C-8M0.2-0.25, Fig.8(e)], it is found that the bending moment shared by the built-in reinforcements of No.5 is smaller than that of No.1, because the strength of the built-in reinforcements of No.5 is smaller than that of No.1.

(4)Influence of the shear reinforcement ratio (p_w)

According to the results of specimens No.1 [p_w=0.2, Fig. 8(a)] and No.6 [p_w=0.1, Fig.8(f)] , it is observed that the shear reinforcement ratio hardly affects the share conditions of the bending moments .

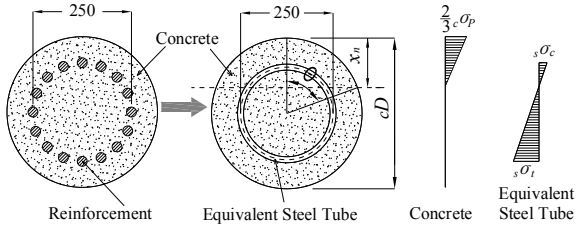

(a) RC section (b)simplified RC section (c)stress distribution

Fig.9 Calculation method and stress distributions for the yield bending strengths of the CFTR column bases

(4) Yield bending strength

a) Calculation method

The cross section of the CFTR column base is the RC section shown in Fig.9(a). Generally, as for the circular RC cross section, the layout of the reinforcements is more complicated than that of the rectangular cross section, hence, the calculations of the bending strengths are more complex than those of the rectangular cross section. As a result, it is common to assume the reinforcements area to the equivalent steel tube[6] [Fig.9(b)]. As shown in Figs.9(a) and (b),the built-in reinforcements are assumed as an equivalent circular steel tube whose sectional area is the same as the area of the total built-in reinforcements. The diameter of the tube wall center circle is taken as 250mm, which is the distance of the center of the reinforcements located in a circle. Hence, in this study, the cross section of the CFTR column base is considered as the simplified RC section shown in Fig.9(b). The stress distributions of the CFTR column bases are also shown in Fig.9(c). Based on the CFT recommendation of AIJ[7], the yield strengths of the CFTR column bases are calculated according to equation 1.

$$\left.\begin{aligned} N &= {}_sN + {}_cN \\ M_y &= {}_sM + {}_cM \end{aligned}\right\} \quad (1)$$

For the concrete, when $x_n \leqq D$:

$${}_cN = \frac{{}_cD^3}{8x_n}\left\{\frac{(\cos^2\theta+2)\sin\theta}{3} - \theta\cos\theta\right\}\cdot\frac{2}{3}{}_c\sigma_p \quad (2)$$

$${}_cM = \frac{{}_cD^4}{64x_n}\left\{\theta + \frac{(\cos^2\theta-5/2)\sin 2\theta}{3}\right\}\cdot\frac{2}{3}{}_c\sigma_p \quad (3)$$

$$\theta = \cos^{-1}(1-2x_n/{}_cD), \qquad {}_c\sigma_p = {}_c\gamma_u\cdot{}_c\sigma_B \quad (4)$$

Where,

x_n : Neutral axis

${}_cD$: Diameter of the concrete

${}_cr_u$: Concrete strength reduction factor(=1.0)

Table 4 Experimental and calculated results of the yield bending strengths

Specimen		n	$M_{y.cal}$	$M_{y.exp}$	$M_{y.exp}/M_{y.cal}$
No.1	C-16M 0.2-0.25	0.25	196	210	1.07
No.2	C-16M 0.2-0.45	0.45	152	238	1.56
No.3	C-16M 0.2-0.10	0.10	232	202	0.87
No.4	C-16H 0.2-0.45	0.45	199	298	1.50
No.5	C-8M 0.2-0.25	0.25	133	153	1.15
No.6	C-16M 0.1-0.25	0.25	233	220	0.94

${}_c\sigma_B$: Concrete cylinder strength

For the equivalent steel tube:

$$\left|\frac{{}_sN}{{}_sA}\right|+\left|\frac{{}_sM}{{}_sZ}\right|={}_s\sigma'_y \tag{5}$$

${}_sA$: Sectional area of the equivalent tube

${}_sZ$: Section modulus of the equivalent tube

${}_s\sigma'_y$: Yield strength of the equivalent tube

b) Results and investigations

Table 4 shows the results of the calculated yield bending strengths $M_{y.cal}$ and the experimental yield bending strengths $M_{y.exp}$. The yield bending strength $M_{y.exp}$ is defined as the strength when the tangent stiffness is 1/3 of the initial stiffness in the M-θ curve (Slope Factor Method).

As listed in Table 4, the ratios $M_{y.exp}/M_{y.cal}$ are from 0.87 to 1.56 (average value is 1.18). With regard to specimens with axial force ratio of 0.10 and 0.25, the $M_{y.exp}/M_{y.cal}$ are from 0.87 to 1.15, which means the experimental yield strengths can be properly evaluated. However, for specimens with axial force ratio of 0.45, the $M_{y.exp}/M_{y.cal}$ are 1.50 and 1.56, which means the experimental yield strengths are a little bit underestimated. The reason for this still need to be further investigated.

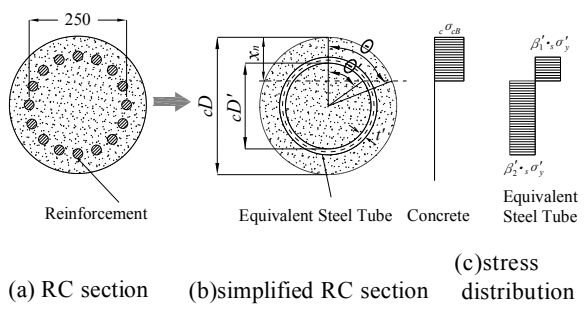

Fig.10 Stress distributions of CFTR column bases for ultimate bending strengths

(5) Ultimate bending strength

a)Calculation for the CFTR Column bases

The cross section of the CFTR column base is consisted of the concrete and the equivalent steel tube, as shown in Fig.10(b). The stress distributions of the concrete and the equivalent steel tube in the ultimate condition are shown in Fig.10(c). Based on the CFT recommendation of AIJ[7], the M-N interactions of the CFTR column bases are calculated according to equation 6. In the calculation, the section is considered under the full plastic condition and the confined effect caused by the steel tube(ϕ 390 × 4) is adopted.

$$\left.\begin{aligned} N_u &= {}_cN_u+{}_sN_u \\ M_u &= {}_cM_u+{}_sM_u \end{aligned}\right\} \tag{6}$$

For the concrete

$${}_cN_u=r_1^2(\theta-\sin\theta\cos\theta)\,{}_c\sigma_{cB} \tag{7}$$

$${}_cM_u=\frac{2}{3}r_1^3\sin^3\theta\cdot{}_c\sigma_{cB} \tag{8}$$

$${}_c\sigma_{cB}={}_c\gamma_u\cdot{}_c\sigma_B+0.78\frac{2t}{D-2t}\,{}_s\sigma_y \tag{9}$$

$$\theta=\cos^{-1}(1-2x_n/{}_cD) \qquad r_1=\frac{{}_cD}{2} \tag{10}$$

For the equivalent steel tube

$${}_sN_u=2r_2t'\{\beta'_1\theta'-\beta'_2(\theta'-\pi)\}\,{}_s\sigma'_y \tag{11}$$

$${}_sM_u=2r_2^2t'(\beta'_1-\beta'_2)\sin\theta'\cdot{}_s\sigma'_y \tag{12}$$

$$\theta'=\cos^{-1}\{({}_cD-2x_n)/{}_cD'\} \qquad r_2=\frac{{}_cD'+t'}{2} \tag{13}$$

$$\beta'_1=1.0 \qquad \beta'_2=-1.0$$

Where

x_n : Neutral axis

D : Diameter of the steel tube(ϕ 390 × 4)

${}_cD$: Diameter of the concrete

t : Wall thickness of the steel tube(ϕ 390 × 4)

t' : Wall thickness of the equivalent steel tube

${}_c\sigma_B$: Concrete cylinder strength

${}_s\sigma_y$: Yield strength of the steel tube(ϕ 390 × 4)

${}_s\sigma'_y$: Yield strength of the equivalent steel tube

${}_cr_u$: Concrete strength reduction factor(=1.0)

b) Calculation for the CFT column

The CFT column cross section without built-in reinforcements is shown in Fig.11, where the stress distributions of the infilled concrete and the steel tube(ϕ 390 × 4) are also indicated. The M-N interactions of the CFT columns (without built-in reinforcements) are calculated according to the CFT recommendation

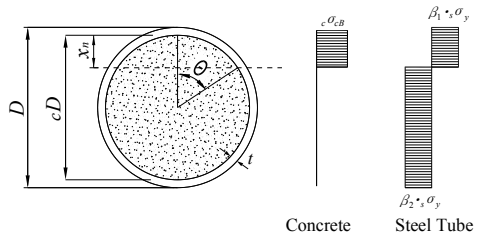

Fig.11 Stress distributions of the CFT columns for the ultimate strengths

of AIJ[7]. The CFT cross section is considered to be in the full-plastic condition. The confined effect is adopted in the calculation.

c) Investigations

Figs.12(a)-(f) show the *M-N* interactions of the experiments and calculations of the ultimate bending strengths. In the figures, the dashed curves imply the calculated *M-N* interactions of the CFTR column bases and the solid curves imply the calculated *M-N* interactions of the CFT columns. Also, the experimental bending strengths at the amplitude of *R*=1.0%, 1.5% and 2.0% are plotted in Fig. 12.

From the relationships between the ultimate bending strengths of the CFT columns and CFTR column bases shown in Fig.12, it is observed that with respect to all specimens, except No.5 [C-8M0.2-0.25,Fig.12(e)], the ultimate strengths of the CFT columns are almost the same to those of the CFTR column bases, which implicates that the CFTR column bases works as the fixed supports for the CFT columns. As for specimen No.5, since the strength of the built-in reinforcements is small, the ultimate strength of the CFT column exceeds that of the CFTR column base.

Also, it is indicated that the experimental bending strengths reaches the calculated strengths of the CFTR column bases when *R* is around 1.0% -1.5% for all specimens.

5. CONCLUSIONS

An experimental study was carried out on the non base-plate type circular CFTR column bases. The following conclusions can be drawn from this study:

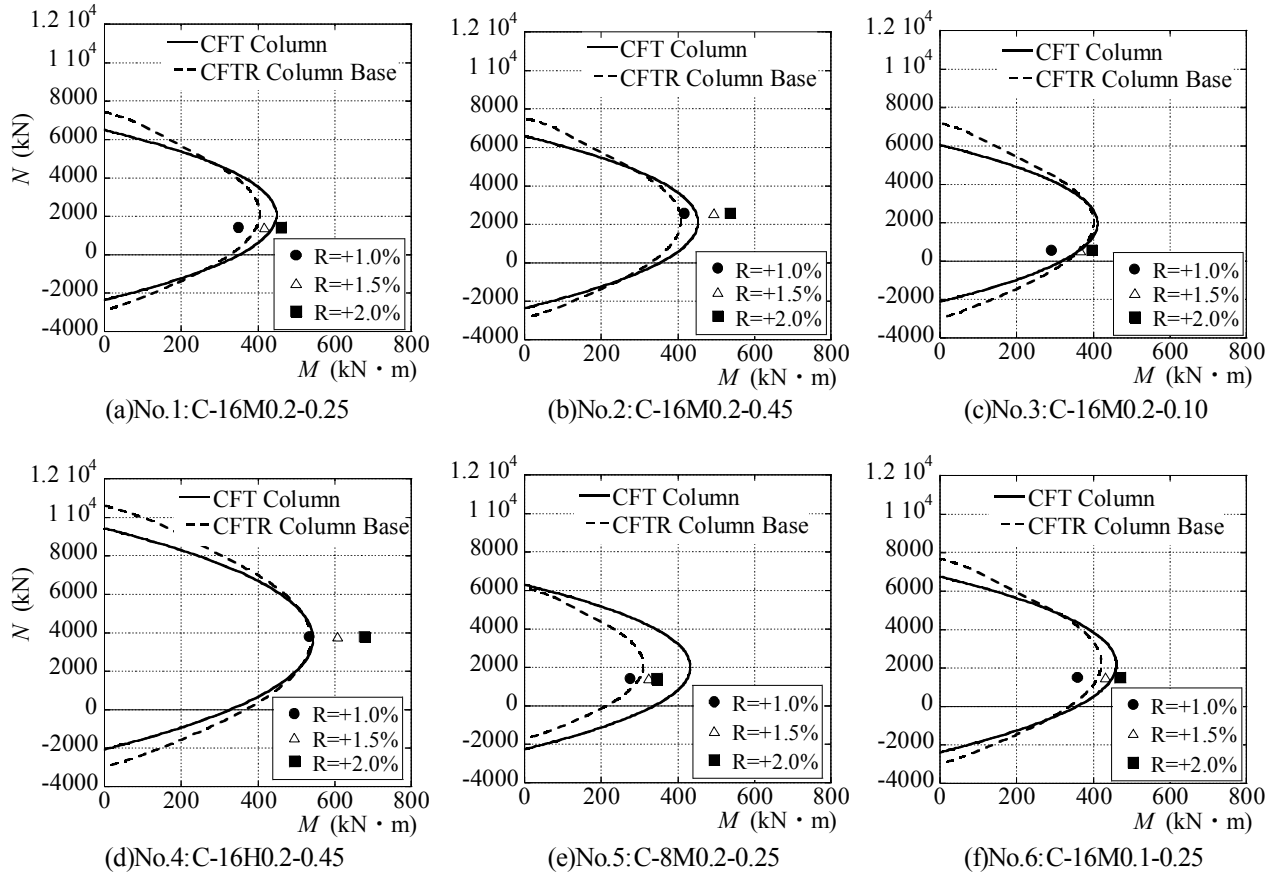

(a)No.1:C-16M0.2-0.25 (b)No.2:C-16M0.2-0.45 (c)No.3:C-16M0.2-0.10

(d)No.4:C-16H0.2-0.45 (e)No.5:C-8M0.2-0.25 (f)No.6:C-16M0.1-0.25

Fig.12 *M-N* interactions of experiments and calculations for the ultimate bending strengths

(1)The specimens show the slip-hysteretic characteristics, but the hysteretic loops are stable and no degradation of the bending moments occurs even when the θ is 5.0%. The non base-plate type circular CFTR column bases proposed are proved having excellent deformation capacities.

(2) The stability of the hysteretic loops and the fracture mode are hardly affected by the differences in the axial force ratios, concrete strengths, built-in reinforcements and shear reinforcement ratios.

(3) According to the share conditions of the bending moments, it is confirmed that the reinforcements and rib plates play the main role in the stress transfer and the stress can be transferred from the steel tube to the foundation in a convincing way.

(4) The yield bending strengths of the CFTR column bases are evaluated by assuming the reinforcements as the equivalent steel tube.

(5) The experimental strengths reaches the calculated ultimate strengths of the CFTR column bases when R is around 1.0%-1.5%.

From above, the non base-plate type circular CFTR column bases proposed in this study are proved to have excellent seismic performances and are applicable in practical structural design.

ACKNOWLEDGEMENTS: The authors would like to thank H.Kubotera(Technical staff of Kyushu University), A. Nawa and F. Kuroki (Former students of Kyushu University), for their help during the experiment.

Also, the authors appreciate the advices from T. Ninakawa (Professor of Kyushu University) and S. Matsuo(Assistant Professor of Kyushu University).

REFERENCES

1) Yamauchi, S., et al. : Empirical Study on Concrete Filled Steel Tube with Built-in Reinforcing Bars , Part1 ~ Part3, Summaries of technical papers of Annual Meeting C-1, AIJ, pp.1199-1204, 2003 (in Japanese)

2) Iwaoka, S., et al. : Experiment on Column of Concrete Filled Steel Tube Built in Reinforcing Bars , Part1 ~ Part2, Summaries of technical papers of Annual Meeting C-1, AIJ, pp. 1173-1176, 2007 (in Japanese)

3) Qiao, Q.Y., et al. : A Study on the Connection of Concrete Filled Steel Tubes (CFT) with built-in Steel Bars, Proceedings of the Sixth International Conference On Behaviour of Steel Structures in Seismic Areas (STESSA 2009), Philadelphia, pp. 319-324, 2009

4) Qiao, Q.Y., et al. : Pure Bending Test on square concrete Filled Steel Tube with Built-in high strength Reinforements(CFTR)Column Joint, Proceedings of the 4th International Conference on Steel & Composite Structures, Sydney, 2010 (CD-rom)

5) Qiao, Q.Y., et al. :Experimental Study on Mechanical Behavior of Square CFT Column Base with Built-in Reinforcements, Proceedings of the ninth Pacific Structural Steel Conference , Beijing, pp. 806-814, 2010.10

6) Cosenza E., et al. : A simplified method for flexural capacity assessment of circular RC cross-sections, Engineering Structures, 33, pp. 942-946, 2011

7) AIJ: Recommendations for Design and Construction of Concrete Filled Steel Tubular Structures, 2008 (in Japanese)